International Journal of Mechanical, Industrial and Aerospace Sciences
ISSN: 2517-9950
Vol:14, No:12, 2020

Performance Prediction of a SANDIA 17-m Vertical Axis Wind Turbine Using Improved Double Multiple Streamtube

Abolfazl Hosseinkhani, Sepehr Sanaye

***Abstract*—**Different approaches have been used to predict the performance of the vertical axis wind turbines (VAWT), such as experimental, computational fluid dynamics (CFD), and analytical methods. Analytical methods, such as momentum models that use streamtubes, have low computational cost and sufficient accuracy. The double multiple streamtube (DMST) is one of the most commonly used of momentum models, which divide the rotor plane of VAWT into upwind and downwind. In fact, results from the DMST method have shown some discrepancy compared with experiment results; that is because the Darrieus turbine is a complex and aerodynamically unsteady configuration. In this study, analytical-experimental-based corrections, including dynamic stall, streamtube expansion, and finite blade length correction are used to improve the DMST method. Results indicated that using these corrections for a SANDIA 17-m VAWT will lead to improving the results of DMST.

***Keywords*—**Vertical axis wind turbine, analytical, double multiple streamtube, streamtube expansion model, dynamic stall model, finite blade length correction.

NOMENCLATURE

c	Blade chord (m)
C_D	Blade section drag coefficient (-)
C_L	Blade section lift coefficient (-)
$C_{L'}$	Modified blade section lift coefficient (-)
$C_{D'}$	Modified blade section drag coefficient (-)
C_N	Blade section normal force coefficient (-)
C_P	Rotor power coefficient (-)
C_Q	Rotor torque coefficient (-)
C_T	Blade section tangential force coefficient (-)
f_{up}, f_{dw}	Upwind and downwind functions (-)
H	Half-height of the rotor (m)
N	Number of blades (-)
R	Rotor radius at equator (m)
Re_b	Blade Reynolds number (-)
S	Rotor swept area (m^2)
s	[Ncl/S] Rotor solidity (-)
u, u′	Upwind and downwind interference factors (-)
V, V′	Upwind and downwind induced velocity (m/s)
V_e	Induced equilibrium velocity (m/s)
V_∞	Wind velocity at equator level (m/s)
W, W′	Upwind and downwind relative inflow velocity (m/s)
X_{EQ}	[Rω/ V_∞] Tip-speed ratio at equator (-)
z	Local turbine height (m)
α, α ′	Upwind and downwind local angle of attack (degree, Âº)
α_w	Atmospheric wind shear exponent (-)
β	Rotor maximum diameter/height ratio (-)
δ	Angle between the blade normal and the equatorial plane (degree, Âº)
θ	Azimuthal angle (degree, Âº)
ρ_∞	Freestream density (kg/m^3)
η	[r/R] Nondimensional Cartesian coordinate (-)
ζ	[z/H] Nondimensional Cartesian coordinate (-)
μ	[2H/c] Blade aspect ratio (-)

A. Abolfazl Hosseinkhani is with Energy Systems Improvement Laboratory, Mechanical Engineering Department, Iran University of Science and Technology, Tehran, Iran (corresponding author, phone: +989134937358; e-mail: a_hosseinkhani@mecheng.iust.ac.ir).

Prof. S. B. Sepehr Sanaye is head faculty, Energy Systems Improvement Laboratory, Mechanical Engineering Department, Iran University of Science and Technology, Tehran, Iran (e-mail: sepehr@iust.ac.ir).

I. INTRODUCTION

DUE to the increasing need for energy and the limitation of fossil resources, attention and use of renewable resources has been recently increased. Wind is one of the most important renewable energies [1]-[4]. Generally horizontal and vertical axis wind turbines are used to extract the kinetic energy of wind. Horizontal axis wind turbines (HAWT) are most commonly used type of turbines because they have high efficiency [5], [6]. Recently VAWT are in the center of attention because of their low cost of maintaining and manufacturing, grounded generator, no need to yaw system etc. [7]-[11]. Because of the growing attention towards VAWTs the performance prediction of these types of wind turbines is important, therefore, several approaches have been considered for this purpose [12]-[18]. The analytical methods, especially momentum models because of some features such as low computational cost, are the most common tool for performance prediction of VAWT. The DMST is one branch of momentum models which divide the plane of rotor into upwind and downwind so the velocity changes through the rotor [19], [20]. Due to complexity of the wind flow through the rotor and strong unsteady characteristics, results from a DMST method differ from experiment [9], [20]. In this study dynamic stall model, streamtube expansion correction and finite blade length correction are used to improve a DMST approach. Results indicated that using these corrections together will improve the performance prediction.

II. DOUBLE MULTIPLE STREAMTUBE MODEL

The DMST considers the swept volume of the rotor by dividing into a series of streamtubes and the VAWT is replaced by two rotor halves in upwind and downwind, which are independent of each other. The governing equations for the

analysis of a Darrieus VAWT are as below.

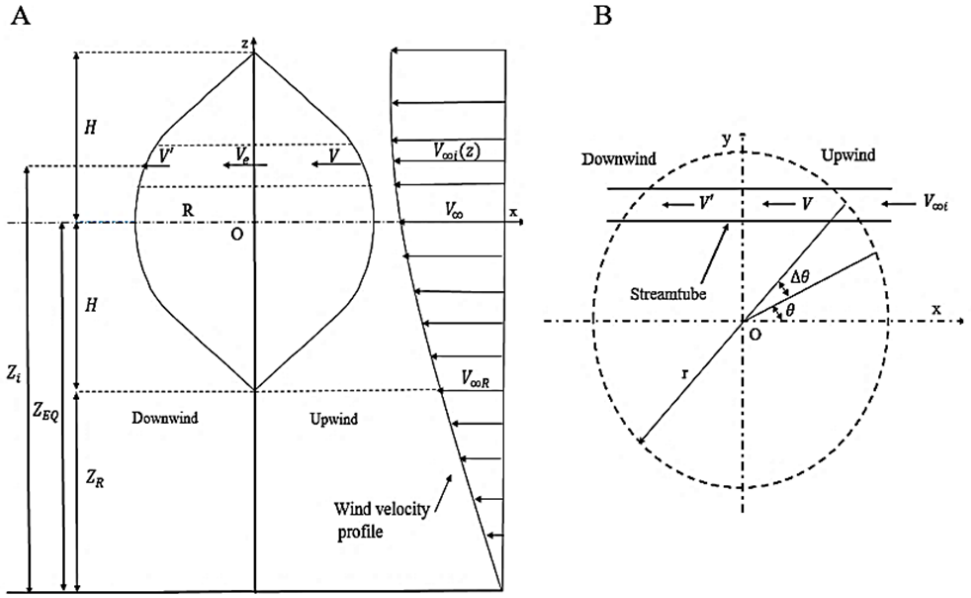

Fig. 1 Definition of rotor geometry for a Darrieus VAWT (A) and schematic of stream tube model (B)

In general, the freestream velocity profile is not uniform but differs with the height as [19]-[21]:

$$V_{\infty i}/V_{\infty} = (Z_i/Z_{EQ})^{\alpha_w} \quad (1)$$

in which α_w is atmospheric wind shear exponent, and can be considered to be 0.1. For the upstream half of the rotor:

$$V = uV_{\infty i} \quad (2)$$

The equilibrium-induced velocity is:

$$V_e = (2u-1)V_{\infty i} \quad (3)$$

and finally for the downwind half of the rotor:

$$V' = u'(2u-1)V_{\infty i} \quad (4)$$

The local relative velocity for the upstream half of the rotor $-\pi/2 \leq \theta \leq \pi/2$ is:

$$W^2 = V^2[(X-\sin\theta)^2 + \cos^2\theta\cos^2\delta] \quad (5)$$

where $X = r\omega/V$ and δ is angle between the blade normal and the equatorial plane. The expression for the local angle of attack is derived as:

$$\alpha = \sin^{-1}\left[\frac{\cos\theta\cos\delta}{\sqrt{(X-\sin\theta)^2+\cos^2\theta\cos^2\delta}}\right] \quad (6)$$

The normal and tangential force coefficient for upwind are:

$$C_N = C_L\cos\alpha + C_D\sin\alpha \quad (7)$$

$$C_T = C_L\sin\alpha - C_D\cos\alpha \quad (8)$$

The torque produced by a blade element is calculated at the center of each element. Integrating along the blade, one obtains the torque on a complete blade as a function of the blade position θ:

$$T_{up}(\theta) = 0.5\rho_{\infty}cRH\int_{-1}^{1} C_T W^2(\eta/\cos\delta)d\zeta \quad (9)$$

The average half-cycle of the rotor torque produced by $N/2$ of the N blades is thus given by:

$$\bar{T}_{up} = \frac{N}{2\pi}\int_{-\pi/2}^{\pi/2} T_{up}(\theta)d\theta \quad (10)$$

and the average half-torque coefficient by the upwind half-cycle of the rotor and the power coefficient can be written as:

$$\bar{C}_{Q1} = \bar{T}_{up}/(\tfrac{1}{2}\rho_{\infty}V_{\infty}^2SR) \quad (11)$$

$$C_{p1} = (R\omega/V_{\infty})\bar{C}_{Q1} = X_{EQ}\bar{C}_{Q1} \quad 12)$$

The governing equations for downwind half of the rotor $\pi/2 \leq \theta \leq 3\pi/2$ are:

$$W'^2 = V'^2[(X'-\sin\theta)^2 + \cos^2\theta\cos^2\delta] \quad (13)$$

$$\alpha' = \sin^{-1}\left[\frac{\cos\theta\cos\delta}{\sqrt{(X'-\sin\theta)^2+\cos^2\theta\cos^2\delta}}\right] \quad (14)$$

The same as upwind half of the rotor for downwind half the equations are as:

$$T_{dw}(\theta) = 0.5\rho_\infty cRH \int_{-1}^{1} C'_T W'^2(\eta/\cos\delta)d\zeta \quad (15)$$

$$\bar{T}_{dw} = \frac{N}{2\pi}\int_{\pi/2}^{3\pi/2} T_{dw}(\theta)d\theta \quad (16)$$

$$\bar{C}_{Q2} = \bar{T}_{dw}/(\tfrac{1}{2}\rho_\infty V_\infty^2 SR) \quad (17)$$

$$C_{p2} = (R\omega/V_\infty)\bar{C}_{Q2} = X_{EQ}\bar{C}_{Q2} \quad (18)$$

and finally, the output power of the turbine is as:

$$\mathrm{P} = \tfrac{1}{2}\rho_\infty \mathrm{V}_\infty^3 \mathrm{S} * (\mathrm{C_{p1}} + \mathrm{C_{p2}}) \quad (19)$$

The DMST model is used to measure the output power of a SANDIA 17-m, the characteristic of this turbine is summarized in Table I. All results are reported for power output against free stream velocity. As can be seen in Fig. 2, the predicted output power of the DMST model without any correction (DMST standard) is differ from experiment data.

TABLE 1
CHARACTERISTIC OF WIND TURBINE

	Sandia 17-m
Rotor geometry	Sandia
Rotational speed (rpm)	42.2
Solidity	0.157
Radius (m)	8.364
Diameter/Height ratio (β)	0.984
C (m)	0.61
Number of blades	2
Airfoil	NACA 0015

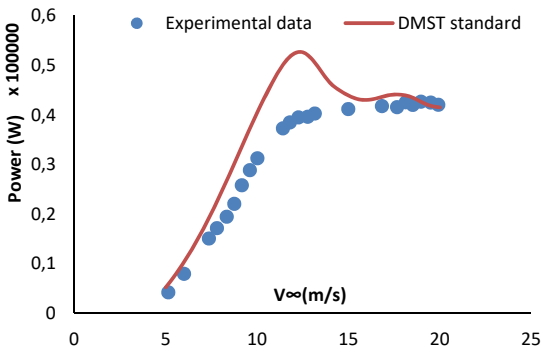

Fig. 2 Comparison of the output power of Sandia 17-m for standard DMST (red line) and experimental data (blue dots)

III. Streamtube Expansion Model

The Darrieus VAWT is a complex and unsteady configuration; within each streamtube of this kind of turbine, the flow diverges toward the downwind half because the velocity decreases, causing the streamtube to expand. In the original DMST model there was no streamtube expansion; in reality, the streamtube upstream of the rotor and downstream in the wake regime should enlarge, which leads to a large portion of the upwind velocity being lost and velocity entering the downwind half of the rotor being highly distorted. Therefore, the interference factor can be corrected from the estimated enlargement factor. For the upstream half of the rotor, the induction factor corrected is [22], [23]:

$$u = \frac{1}{2}[1 + (2u_0 - 1)(2u_{n-1} - 1)] \quad (20)$$

and the induction factor corrected for downwind is:

$$u' = \frac{1}{2}[1 + (2u'_0 - 1)(2u'_{n-1} - 1)] \quad (21)$$

where k_0 is the interference factor without streamtube expansion, and k_{n-1} is interference factor obtained from the previous iteration.

Fig. 3 shows the DMST model with using streamtube expansion model correction in comparison with experiment data. As can be seen in this figure, the results have good agreement with experimental data; however, there is still a slight difference that the following sections attempt to improve the results.

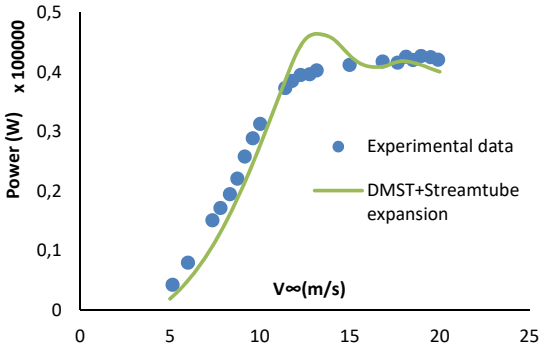

Fig. 3 Comparison of the output power of Sandia 17-m for standard DMST+ streamtube expansion model (green line) and experimental data (blue dots)

IV. Dynamic Stall Model

Dynamic stall is an unsteady and complex phenomenon that is related to a large and rapid change of angle of attack. Under such the condition lift and drag characteristic presents a hysteresis response. Gormont's model considers the hysteresis model by defining a reference angle of attack which is different from geometric angle of attack; this reference angle is given by:

$$\alpha_{ref} = \alpha - K_1\Delta\alpha \quad (22)$$

where:

$$K_1 = \begin{cases} 1 & when\ \dot{\alpha} \geq 0 \\ -0.5 & when\ \dot{\alpha} < 0 \end{cases} \quad (23)$$

$$\Delta\alpha = \begin{cases} \gamma_1 S & when\ S \leq S_c \\ \gamma_1 S_c + \gamma_2(S - S_c) & when\ S > S_c \end{cases} \quad (24)$$

$$S = \sqrt{\left|\frac{c\dot{\alpha}}{2W}\right|}, \quad S_c = 0.06 + 1.5\left(0.06 - {}^{t}/_{c}\right) \quad (25)$$

$$\gamma_1 = \begin{cases} \frac{\gamma_2}{2} & \text{for lift characteristic} \\ 0 & \text{for drag characteristic} \end{cases} \quad (26)$$

$$\gamma_2 = \gamma_{max}\, max\left\{0, \min[1, \frac{M-M_2}{M_1-M_2}]\right\} \quad (27)$$

where $\dot{\alpha}$ is the time derivative of α, M is the Mach number, and t/c is the airfoil relative thickness. The expressions for γ_{max}, M_1 and M_2 are in Table II. Finally, for Gormont's model the dynamic coefficients are given by:

$$C_L^{dyn} = C_L(\alpha_0) + m(\alpha - \alpha_0) \quad (28)$$

$$C_D^{dyn} = C_D(\alpha_{ref}) \quad (29)$$

where:

$$m = min\left[\frac{C_L(\alpha_{ref})-C_L(\alpha_0)}{\alpha_{ref}-\alpha_0}, \frac{C_L(\alpha_{ss})-C_L(\alpha_0)}{\alpha_{ss}-\alpha_0}\right] \quad (30)$$

In this equation, α_{ss} is the static-stall angle of attack and α_0 is any convenient angle of attack. Note that in this model, the value of the reference angle of attack differs for drag and for lift.

TABLE II
DEFINITIONS OF M_1, M_2 AND γ_{max}

	Lift characteristic	Drag characteristic
M_1	0.4+5.0(0.06-t/c)	0.2
M_2	0.9+2.5(0.06-t/c)	0.7+2.5(0.06-t/c)
γ_{max}	1.4+6.0(0.06-t/c)	1.0+2.5(0.06-t/c)

The Gormont's model was developed for helicopter blades, and this model over predicts the effect of dynamic stall. In this study for considering the effect of dynamic stall, the modification presented by [24] is used, and the expression is presented as [22]:

$$C_L^{mod} = \begin{cases} C_L + \left[\frac{A_M\alpha_{ss}-\alpha}{A_M\alpha_{ss}-\alpha_{ss}}\right](C_L^{dyn} - C_L), & when\ \alpha \le A_M\alpha_{ss} \\ C_L, & when\ \alpha > A_M\alpha_{ss} \end{cases} \quad (31)$$

$$C_D^{mod} = \begin{cases} C_D + \left[\frac{A_M\alpha_{ss}-\alpha}{A_M\alpha_{ss}-\alpha_{ss}}\right](C_D^{dyn} - C_D), & when\ \alpha \le A_M\alpha_{ss} \\ C_D, & when\ \alpha > A_M\alpha_{ss} \end{cases} \quad (32)$$

A_M is an empirical constant, [24] has proposed the use of $A_M = 6$. The results of using dynamic stall model are shown in Fig. 4. As can be seen in Fig. 4, the current dynamic stall model can improve the output power for SANDIA 17-m in comparison with the standard DMST.

V. Finite Blade Length Correction

Blade aerodynamic data are generally provided based on infinite blade length (two-dimensional flow approximations). In order to accurately model VAWTs with finite blade length, the aerodynamic coefficients should be modified considering the effect of finite blade length. The modified lift and drag for a finite length can be estimated from (33) and (34) [25], from which an increase in drag and a decrease in lift coefficients can be inferred. The results are given in Fig. 5, as can be seen the results are slightly closer to the experimental results. Note that the effect of finite blade length correction is less than the other corrections.

$$C_L' = \frac{C_L}{1+\frac{\alpha_0}{\pi\mu}} \quad (33)$$

$$C_D' = C_D + \frac{C_L^2}{\pi\mu} \quad (34)$$

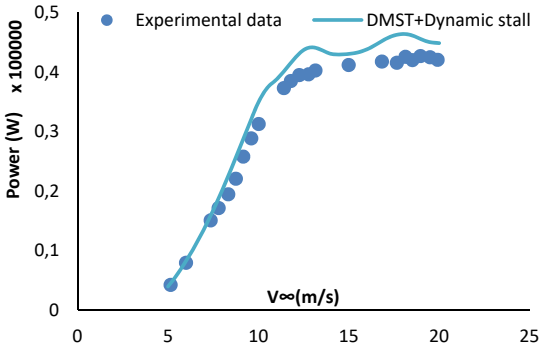

Fig. 4 Comparison of the output power of Sandia 17-m for standard DMST+ dynamic stall model (blue line) and experimental data (blue dots)

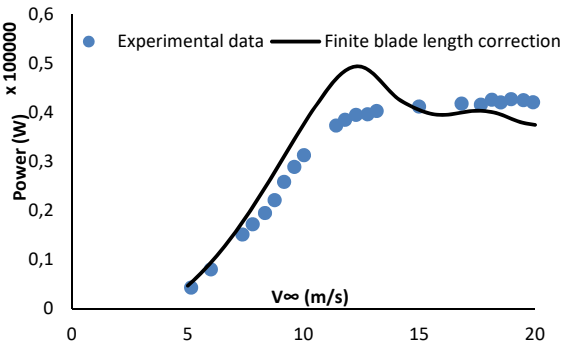

Fig. 5 Comparison of the output power of Sandia 17-m for standard DMST+ finite blade length correction (black line) and experimental data (blue dots)

VI. Combining the Correction Models

In this section, three correction models are combined and the results are given in Fig. 6. As can be seen in this figure, there is significant agreement between the results and the experimental data. It can be concluded that the combination of the dynamic stall model, the streamtube expansion and finite blade length correction can improve the accuracy of the performance prediction.

VII. Conclusion

In this study, a DMST model was used to predict the performance of a SANDIA 17-m VAWT (the characteristic of this turbine is presented in Table I). Our findings highlighted

that the results obtained from a standard DMST model without any correction have differed from experimental data. Therefore, three analytical-experimental-based corrections are used including the streamtube expansion model, the dynamic stall model (modification of Berg [24]) and the finite blade length correction. Initially, each model was implemented separately. The results shown are slightly in agreement with the experimental data but there were still some differences. Finally, when three correction models were applied simultaneously, the results showed greater accuracy with experimental data.

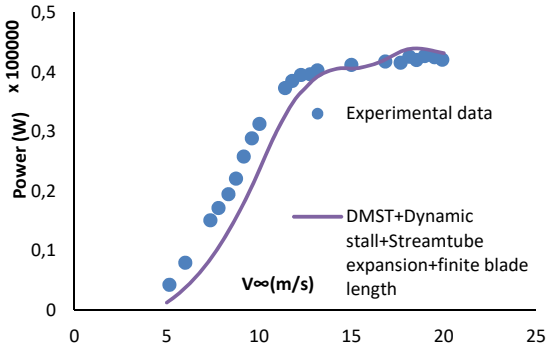

Fig. 6 Comparison of the output power of Sandia 17-m for standard DMST+ dynamic stall model + streamtube expansion + finite blade length correction (purple line) and experimental data (blue dots)

REFERENCES

[1] S. L. Dixon and C. A. Hall, *Wind Turbines*. 2010.
[2] A. ElCheikh, M. Elkhoury, T. Kiwata, and T. Kono, "Performance analysis of a small-scale Orthopter-type Vertical Axis Wind Turbine," *J. Wind Eng. Ind. Aerodyn.*, vol. 180, no. July, pp. 19–33, 2018.
[3] P. Jain and A. Abhishek, "Performance prediction and fundamental understanding of small scale vertical axis wind turbine with variable amplitude blade pitching," *Renew. Energy*, vol. 97, pp. 97–113, 2016.
[4] M. Khalid Saeed, A. Salam, A. U. Rehman, and M. Abid Saeed, "Comparison of six different methods of Weibull distribution for wind power assessment: A case study for a site in the Northern region of Pakistan," *Sustain. Energy Technol. Assessments*, vol. 36, no. May, p. 100541, 2019.
[5] Z. Zhao *et al.*, "Study on variable pitch strategy in H-type wind turbine considering effect of small angle of attack," *J. Renew. Sustain. Energy*, vol. 9, no. 5, 2017.
[6] I. Hui, B. E. Cain, and J. O. Dabiri, "Public receptiveness of vertical axis wind turbines," *Energy Policy*, vol. 112, no. October 2017, pp. 258–271, 2018.
[7] G. E. Brandvold, "Vertical Axis Wind Turbine Status," *Sun Mankind's Futur. Source Energy*, no. October, pp. 1843–1847, 2013.
[8] M. Douak, Z. Aouachria, R. Rabehi, and N. Allam, "Wind energy systems: Analysis of the self-starting physics of vertical axis wind turbine," *Renew. Sustain. Energy Rev.*, vol. 81, no. March, pp. 1602–1610, 2018.
[9] G. Bangga, T. Lutz, A. Dessoky, and E. Krämer, "Unsteady Navier-Stokes studies on loads, wake, and dynamic stall characteristics of a two-bladed vertical axis wind turbine," *J. Renew. Sustain. Energy*, vol. 9, no. 5, 2017.
[10] Q. Li, T. Maeda, Y. Kamada, Y. Hiromori, A. Nakai, and T. Kasuya, "Study on stall behavior of a straight-bladed vertical axis wind turbine with numerical and experimental investigations," *J. Wind Eng. Ind. Aerodyn.*, vol. 164, no. February, pp. 1–12, 2017.
[11] K. H. Wong, W. T. Chong, N. L. Sukiman, S. C. Poh, Y. C. Shiah, and C. T. Wang, "Performance enhancements on vertical axis wind turbines using flow augmentation systems: A review," *Renew. Sustain. Energy Rev.*, vol. 73, no. June 2016, pp. 904–921, 2017.
[12] H. Y. Peng, H. F. Lam, and H. J. Liu, "Power performance assessment of H-rotor vertical axis wind turbines with different aspect ratios in turbulent flows via experiments," *Energy*, 2019.
[13] W. Wang, J. Wang, and W. T. Chong, "The effects of unsteady wind on the performances of a newly developed cross-axis wind turbine: A wind tunnel study," *Renew. Energy*, 2018.
[14] Y. Wu, H. Lin, and J. Lin, "Certification and testing technology for small vertical axis wind turbine in Taiwan," *Sustain. Energy Technol. Assessments*, vol. 31, no. November 2018, pp. 34–42, 2019.
[15] J. Kjellin, F. Bülow, S. Eriksson, P. Deglaire, M. Leijon, and H. Bernhoff, "Power coefficient measurement on a 12 kW straight bladed vertical axis wind turbine," *Renew. Energy*, vol. 36, no. 11, pp. 3050–3053, 2011.
[16] Y. Wang, H. Tong, H. Sima, J. Wang, and J. Sun, "Experimental study on aerodynamic performance of deformable blade for vertical axis wind turbine," *Energy*, vol. 181, pp. 187–201, 2019.
[17] L. Battisti *et al.*, "Experimental benchmark data for H-shaped and troposkien VAWT architectures," *Renew. Energy*, vol. 125, pp. 425–444, 2018.
[18] B. Zouzou, I. Dobrev, F. Massouh, and R. Dizene, "Experimental and numerical analysis of a novel Darrieus rotor with variable pitch mechanism at low TSR," *Energy*, vol. 186, p. 115832, 2019.
[19] I. Paraschivoiu, "Aerodynamic Loads and Performance of the Darrieus Rotor.," *J Energy*, vol. V 6, no. N 6, pp. 406–412, 1982.
[20] I. Paraschivoiu and F. Delclaux, "Double multiple streamtube model with recent improvements (for predicting aerodynamic loads and performance of Darrieus vertical axis wind turbines)," *J. Energy*, vol. 7, no. 3, pp. 250–255, 1983.
[21] I. Paraschivoiu, O. Trifu, and F. Saeed, "H-Darrieus wind turbine with blade pitch control," *Int. J. Rotating Mach.*, vol. 2009, 2009.
[22] G. Bangga, A. Dessoky, T. Lutz, and E. Kr, "Improved double-multiple-streamtube approach for H-Darrieus vertical axis wind turbine computations," vol. 182, pp. 673–688, 2019.
[23] "Paraschivoiu I.-Wind Turbine Design_ With Emphasis on Darrieus Concept."
[24] D. E. Berg, "Improved double-multiple streamtube model for the Darrieus-type vertical axis wind turbine," *Sol. Energy Soc*, 1983.
[25] M. Ahmadi-Baloutaki, R. Carriveau, and D. S. K. Ting, "Straight-bladed vertical axis wind turbine rotor design guide based on aerodynamic performance and loading analysis," *Proc. Inst. Mech. Eng. Part A J. Power Energy*, vol. 228, no. 7, pp. 742–759, 2014.